

pubs.acs.org/JPCB Article

Predicting Gaseous Solute Diffusion in Viscous Multivalent Ionic Liquid Solvents

Published as part of The Journal of Physical Chemistry B virtual special issue "COIL-9:9th Congress on Ionic Liquids".

Feranmi V. Olowookere and C. Heath Turner*



Cite This: J. Phys. Chem. B 2023, 127, 9144-9154



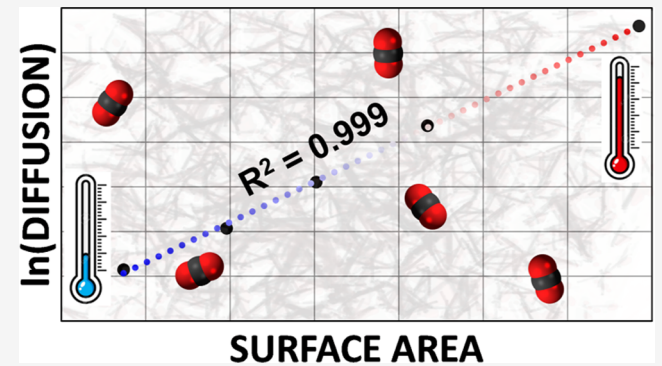
ACCESS

III Metrics & More

Article Recommendations

s Supporting Information

ABSTRACT: Calculating solute diffusion in dense, viscous solvents can be particularly challenging in molecular dynamics simulations due to the long time scales involved. Here, a new scaling approach is developed for predicting solute diffusion based on analyses of CO₂ and SO₂ diffusion in two different multivalent ionic liquid solvents. Various scaling approaches are initially evaluated, including single and separate thermostats for the solute and solvent, as well as the application of the Arrhenius relationship and the Speedy—Angell power law. A very strong logarithmic correlation is established between the solvent-accessible surface area and solute diffusion. This relationship, reflecting Danckwerts' surface renewal theory and the Vrentas—Duda free volume model, presents a valuable method for estimating diffusion behavior from



short simulation trajectories at elevated temperatures. The approach may be beneficial for enhancing predictive modeling in similar challenging systems and should be more broadly evaluated.

1. INTRODUCTION

Diffusion processes are essential to understanding many phenomena in materials science, chemistry, and other fields, including the transport of ions in batteries and fuel cells, ^{1,2} the movement of pollutants in the environment, 3,4 and the behavior of biomolecules in biological systems.⁵ Diffusion plays a critical role in understanding the behavior of molecules and ions and is key to the development of new materials and processes in many industries.^{6–9} In particular, the effectiveness of solvation and separation processes is strongly dictated by transport and diffusion rates, and these are important properties to quantify when screening for new solvent formulations. In recent years, there have been many studies exploring the solvation performance of ionic liquids (ILs) and their gas absorption behavior, 10-14 largely due to their unique characteristics (e.g., high stability, low volatility, tunable selectivity). These properties make ILs a promising alternative to traditional liquid solvents, particularly for gas separation, absorption, and storage applications, 15,16 which are important for addressing the environmental aspects of industrial processes and climate change.

It is crucial to understand the behavior of gas solutes in novel IL solvent formulations, especially during computational screening stages. However, gas diffusion is strongly influenced by the complex interactions between neighboring atoms or molecules, ¹⁷ as well as the thermodynamic operating conditions, making the prediction of solute behavior a challenging task. While there have been many studies ^{18–21} focused on equilibrium gas solvation and selectivity behavior in ILs, there has been much less work focused on describing the solute transport properties, which must be evaluated for any practical application.

The diffusion of solutes in condensed systems has been studied extensively since the pioneering work of Graham²² and Fick,²³ using experimental methods such as nuclear magnetic resonance (NMR),²⁴ Raman microspectroscopy,²⁵ and dynamic light scattering (DLS).²⁶ However, depending on the system, these methods can be expensive, time-consuming, and challenging to perform, especially under unfavorable conditions, such as high temperatures and pressures. To overcome these limitations, theoretical models have been developed based on kinetic theory and hydrodynamics, such as those of Gross,²⁷ Wilke–Chang,²⁸ and Stokes–Einstein.²⁹ However,

Received: June 7, 2023
Revised: September 18, 2023
Published: October 13, 2023





these models have limitations in their ability to predict the performance over a wide range of fluids, and they provide rather inaccurate predictions for nonionized compounds, as their diffusivities tend to be anomalously high. The provide recent studies by Tsimpanogiannis et al. The assessed the experimental and simulation data on intradiffusivities of H_2 and O_2 in H_2O and the self-diffusivity of pure H_2O to test the Stokes–Einstein relation. Findings revealed deviations from the expected values, suggesting that the Stokes–Einstein relation is not consistently valid for these systems; improvements are possible by refining the slope calculations. Recent enhancements to other models (e.g., Darken-based models) have doubled their accuracy in predicting self-diffusion coefficients in nonideal binary liquid mixtures, surpassing the McCarty and Mason correlation.

Molecular dynamics (MD) simulations have become increasingly valuable for studying the diffusion of solutes in dense or viscous systems, especially for gaining insight into the behavior of solutes that is difficult to observe experimentally. The diffusion predictions are typically based on various analyses of the molecular trajectories, such as the mean square displacement (MSD) or the velocity autocorrelation function (VACF), as shown in eqs 1 and 2, respectively. The diffusion coefficient (D_i) of the component i can be determined by averaging the MSDs over time using the Einstein correlation:

$$D_{i} = \frac{1}{6N} \lim_{t \to \infty} \frac{\mathrm{d}}{\mathrm{d}t} \langle |\mathbf{r}_{i}(t) - \mathbf{r}_{i}(0)|^{2} \rangle \tag{1}$$

Alternately, the diffusion coefficient can be calculated as an integral over the VACF, which is based on the correlation between particle velocities at different time increments:

$$D_{i} = \frac{1}{3N} \int_{0}^{\infty} \langle \mathbf{v}(0) \cdot \mathbf{v}(\tau) \rangle d\tau$$
 (2)

The MSD analysis is generally more accurate in viscous systems, as it can capture the diffusion of particles that may not have fully decoupled their velocities. Additionally, the Einstein correlation⁴⁰ can be used to estimate diffusion coefficients, provided the viscosity of the medium in which the solute is diffusing is known. However, it is important to recognize that the solute might alter the viscosity of the fluid, complicating the application of the Einstein correlation. MD simulations can often predict diffusion coefficients with an accuracy of around ±10%, 41,42 depending on the specific system and simulation parameters used; predictions can be compromised by the finite size and periodic boundary effects, among other underlying factors, such as poorly parametrized force fields. For instance, Jamali et al.⁴³ showed a notable dependency of diffusion coefficients on the system size in molecular mixtures, leading to a proposed correction based on factors such as viscosity and system nonideality, which when applied, significantly improves the reliability. For more information on the influence of finite size effects on diffusion coefficients, we refer the reader to a comprehensive review by Celebi et al.44

Many studies have been conducted in the literature using MD simulations to obtain diffusion coefficients of different gases in viscous solvents. Reddy et al., ¹⁸ for instance, studied the structure and dynamics of certain ILs, revealing higher diffusion coefficients from VACFs than from MSDs (using trajectories of over 100–250 ns); they highlighted the decelerating influence of hydroxyalkyl chains on cation dynamics. Building on this, Figueiredo et al. ⁴⁵ employed

MSDs over a 10 ns trajectory to investigate room-temperature ILs (RTILs), as well as their binary mixtures with methanol and ethanol. They observed that reducing the IL composition increases the ion self-diffusion coefficients while inversely affecting the density and viscosity. In addition, MD simulations (using ~20 ns trajectories) have been used to assess the effects of external electric fields (EEFs) on deep eutectic solvents (DESs); the EEFs tend to increase the self-diffusion coefficients while concurrently decreasing the viscosity. Overall, MD simulations have proven to be instrumental in advancing our understanding of key environmental and chemical processes by capturing the diffusion behavior in different IL solvents.

In order to extract a representative diffusion coefficient from MD, it is important to ensure a convergence of the MSD or VACF data, i.e., a linear slope of the MSD versus time and a convergence of the VACF near zero at long times. However, describing diffusion accurately using MD can be a challenging task, particularly in dense and viscous solvents. This can make it difficult to obtain reliable diffusion rates from MD simulation trajectories, which typically range from tens to hundreds of nanoseconds in duration. To accurately represent solute behavior in such systems, it is often necessary to use very long MD trajectories that allow for the exploration of rare events and thoroughly sample the phase space. For instance, in previous simulations of ILs, Tsuzuki²¹ found that at least 10 ns is necessary before observing any behavior similar to diffusion at room temperature. Similarly, Reddy et al., 18 Figueiredo et al., 19 and Jahanbakhsh-Bonab et al. 20 noted MSD evaluations requiring trajectories of 20-300 ns. In some cases, the trajectories may need to be extended for microseconds, leading to severe computational bottlenecks.

Several methods have been devised to enhance the efficiency of MD simulations for diffusion calculations and improve the sampling of the phase space. These techniques include advanced sampling methods such as umbrella sampling (UMS) and metadynamics (MET), which use bias potentials to explore a wide range of configurations in the energy landscape, and accelerated MD (AMD) techniques such as temperature-accelerated MD (TAMD) and hypermolecular dynamics (HMD). For instance, MET has been applied to explore a broad range of energy configurations in alanine dipeptides and amino acids, while AMD has been used to improve the sampling of rare events in simulations of liquid water, including hydrogen bond formation and water diffusion. In Furthermore, recent studies have employed HMD to study self-interstitial diffusion in α -iron.

While these techniques can be useful in some cases, they can also introduce artifacts or bias in the simulation results. In particular, accelerated sampling methods can lead to overrepresentation of rare events or states, which can skew the results of diffusion calculations. Additionally, these methods can still be very computationally demanding, and their implementation is not trivial. For instance, UMS may require the use of multiple simulations or replicas to generate sufficient data for accurate estimation of the diffusion coefficient, which can be particularly challenging when dealing with large or complex systems. On the diffusion coefficient or complex systems.

The diffusion of gas species in ILs is typically attributed to a "hopping" mechanism. ^{56,57} However, the hopping behavior is shown to be non-Arrhenius, a fact that has been frequently identified in the IL literature. ^{58,59} Adding to the complexity, the amorphous nature of ILs introduces significant variability

Figure 1. Chemical structures of the anion (A1 $[NpO_2]^{2-}$) and the two cations (C2 $[Bzmim_3]^{3+}$ and C3 $[Bzmim_4]^{4+}$) composing the ILs simulated in this study.

in these hopping pathways. Furthermore, gas absorption can significantly alter the properties of the IL system, such as a reduction in viscosity and other substantial changes. Thus, it can be very challenging to make theoretical or phenomenological predictions of diffusion behavior. Regardless, the Speedy–Angell power law (eq 3) is often used to correlate simulated diffusion (D_s) results:

$$D_{\rm s} = D_0 \left(\frac{T}{T_{\rm s}} - 1\right)^m \tag{3}$$

where T is temperature and D_0 , $T_{\rm s}$, and m are fitted parameters. Previously, the diffusion coefficient of ${\rm CO}_2$ molecules in the supercritical region has been fit to this power law equation, resulting in good agreement with MD simulation results ($R^2=0.985$). This trend highlights the non-Arrhenius behavior. Nevertheless, this equation has shown limited applicability in other mixtures and at certain supercritical and subcritical regions. 62,63

Here, we examine the diffusion behavior of carbon dioxide (CO₂) and sulfur dioxide (SO₂) in two different multivalent ILs, in an attempt to develop an extrapolation approach for predicting solute diffusion at room temperature conditions, which otherwise requires extremely long trajectories for convergence. Our findings suggest that the accessible surface area of the solvent has a strong logarithmic correlation to solute diffusion rates, which provides a simple and efficient approach for rapidly obtaining diffusion rates in viscous systems (such as ILs at room temperature). We show that as the temperature increases, the liquid expands, and the surface area increases in a predictable manner, creating more space (or windows between adjacent pockets) for the solute molecules to diffuse. This extrapolation approach avoids the need for long trajectories in the systems studied, and it motivates future investigation of its reliability for predicting diffusion in other viscous solvents.

2. METHODS

Quantum chemical (QC) methods were used to refine the intermolecular potentials for our system, while grand canonical Monte Carlo (GCMC) and MD simulations were used to perform the diffusion calculations. The solute concentrations were determined by carrying out a combination of GCMC and MD simulations, which allowed us to obtain well-converged estimates of the gas loading. For a more detailed explanation of the QC calculations and GCMC simulations, we refer the reader to our previous work.⁶⁴

The intermolecular potentials used for the multivalent IL systems in this work have been described previously, 65 and the different ions are illustrated in Figure 1. To initialize the systems, the ion pairs were randomly inserted into the simulation box at a low density using PACKMOL, 66 followed

by MD simulation using Gromacs 5.0.⁶⁷ The number of ions used in the simulations varied based on the system stoichiometry, with the exact compositions summarized in Table 1. The force field parameters for the ionic liquids and

Table 1. Summary of the Simulated IL Properties Composed of the Different Ion Pairs (m = Number of Cation Molecules, n = Number of Anion Molecules, x = Number of Solute Molecules, and $M_w =$ Molecular Weight of ILs), as well as the Average Density of Each System at a Temperature of 300 K and a Pressure of 1 Bar

system	m	n	x	density (g/cm ³)	$M_{\rm w} ({ m g/mol})$	gas solubility (g/L)
SO ₂ -A1C2	648	432	172	1.421	1502	45.6 ± 0.2
SO ₂ -A1C3	432	216	142	1.447	975	58.8 ± 0.3
CO ₂ -A1C2	648	432	133	1.400	1502	25.6 ± 0.2
CO ₂ -A1C3	432	216	105	1.404	975	29.7 ± 0.2

input files are presented in the Supporting Information. The OPLS-AA force field, ⁶⁸ as assigned by LigParGen, ⁶⁹ was used to describe the ion interactions in the system. The molecular parameters for CO₂ were taken from the TraPPE force field provided by Siepmann et al., ⁷⁰ while the SO₂ parameters were taken from Ketko et al. ⁷¹ The simulations were performed in the isothermal–isobaric (NPT) ensemble; the temperature was maintained using the Nosé–Hoover thermostat, ⁷² and the pressure was maintained using the Parrinello–Rahman barostat, ⁷³ with time constants of 0.5 and 1 ps, respectively.

Following an initial relaxation via the steepest-descent algorithm, the system was equilibrated in the NPT ensemble at 300 K and 1 bar for 10 ns using a time step of 1 fs. Subsequently, the production phases were conducted for varying durations, ranging from tens of nanoseconds to several microseconds, depending on the convergence behavior at different temperatures. The Lennard–Jones potential and electrostatic interactions were calculated with a cutoff distance of 1.2 nm, and the particle mesh Ewald (PME) method⁷⁴ was used for long-range electrostatic interaction with 0.12 nm of Fourier spacing. Cross-term interactions between unlike sites were approximated with the Lorentz–Berthelot mixing rules. The bonds with H atoms were constrained using the LINCS method.⁷⁵ Periodic boundary conditions were implemented in all three dimensions.

3. RESULTS AND DISCUSSION

In this section, we present the outcomes of standard MD simulations to calculate gas diffusion coefficients in different multivalent ILs, followed by different scaling approaches (both naive and more effective techniques) for estimating diffusion coefficients under challenging conditions (i.e., low temperatures). Initially, "brute force" MD simulations are used to evaluate the convergence behavior over very long trajectories.

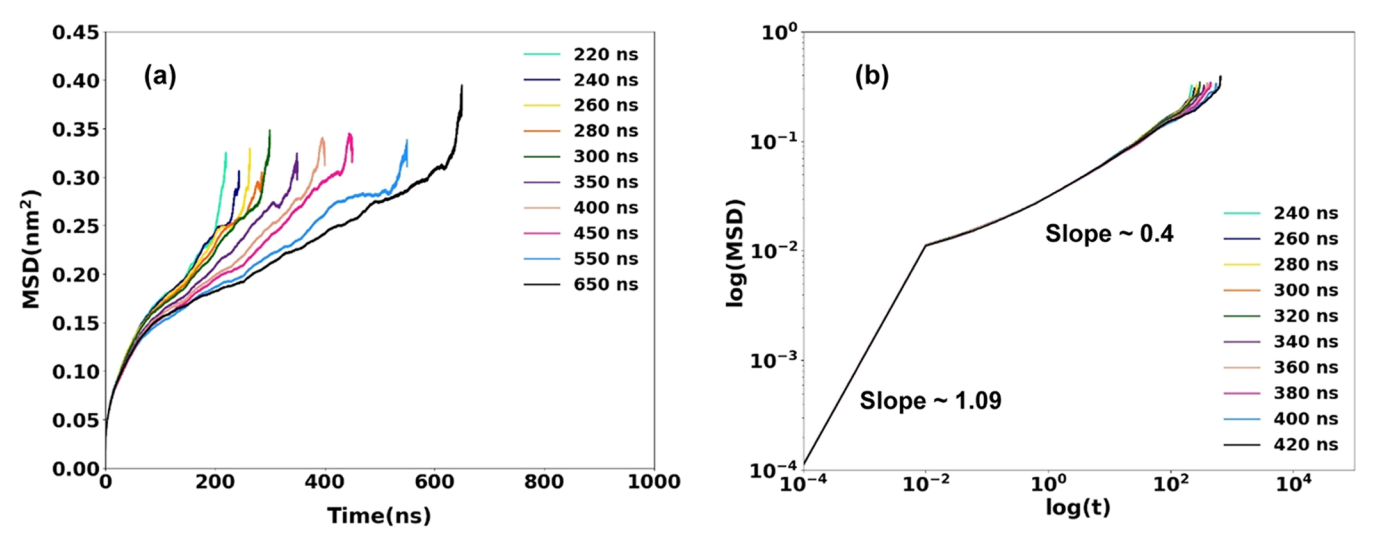


Figure 2. (a) MSD vs time; (b) log MSD vs log t of SO₂ in the A1C3 IL corresponding to different MD trajectory lengths at 300 K.

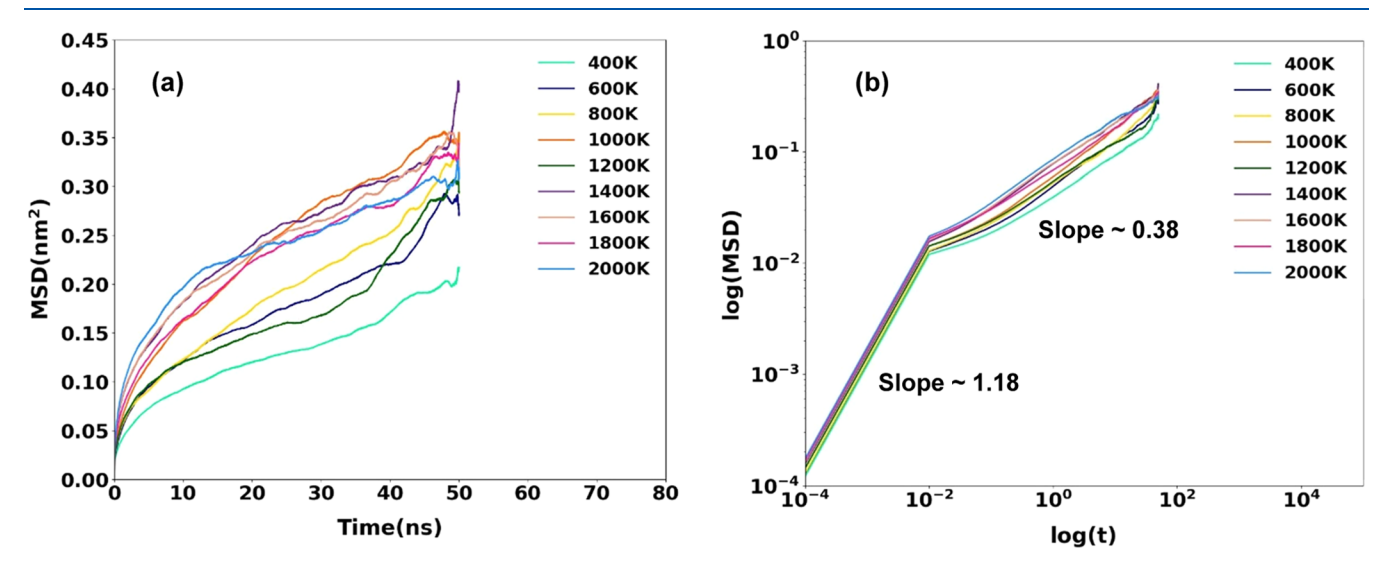


Figure 3. (a) MSD vs time; (b) log MSD vs log t of SO₂ in the A1C3 IL, corresponding to different simulations in which the solute molecule temperatures are elevated (as shown), while the solvent molecules remain near room temperature (300 K) by using separate thermostats, over a 50 ns time frame.

As depicted in Figure 2 (SO₂ in the A1C3 IL), accurate diffusion predictions necessitate extended simulation trajectories. Despite the long simulation times shown in Figure 2, as well as long segments of seemingly converged (linear) behavior, the MSD values indicate that the solutes are relatively stagnant, even over the course of several hundred nanoseconds. On average, the solutes have a net MSD displacement of only ~0.3 nm² (or a linear displacement of \sim 0.55 nm), indicating that the solute traveled only \sim 0.06 box sizes. Thus, the solute diffusion at room temperature is highly restricted in these ILs, requiring a very long trajectory to reach beyond subdiffusive motion. In order to mitigate these challenging dynamics, we test different scaling approaches for predicting the solute diffusion at these conditions, based on simulations at higher temperatures (with inherently faster solute dynamics).

3.1. Separate Temperature Coupling and the Thermal Scaling Behavior of Diffusivity. The first scaling approach is to perform simulations at higher temperatures by using separate thermostats for the solute and solvent. Although

this is unphysical, the strategy is to significantly elevate the solute temperature to incrementally higher values (in different independent simulations) to provide additional kinetic energy for the solutes to hop from one IL domain to a neighboring cavity while the solvent remains fixed at room temperature (300 K). Using the Berendsen thermostat, various solute thermostat parameters were tested, ranging from small to very large time constants as well as small to large temperature increments.

A representative plot of the MSD of the SO_2 molecules in the A1C3 IL is shown in Figure 3, which illustrates the effect of this approach (i.e., implementation of different solute temperatures). Although the displacements of the SO_2 molecules are moderately increased by imposing a higher temperature, even over a duration of 50 ns, the SO_2 molecules do not display significant movement (\sim 0.3 nm²). Furthermore, the different curves do not provide any discernible scaling behavior over the range of temperatures tested, preventing the development of predictive correlations. The same slow, spurious behavior is also observed when simulating CO_2 solutes within the A1C3

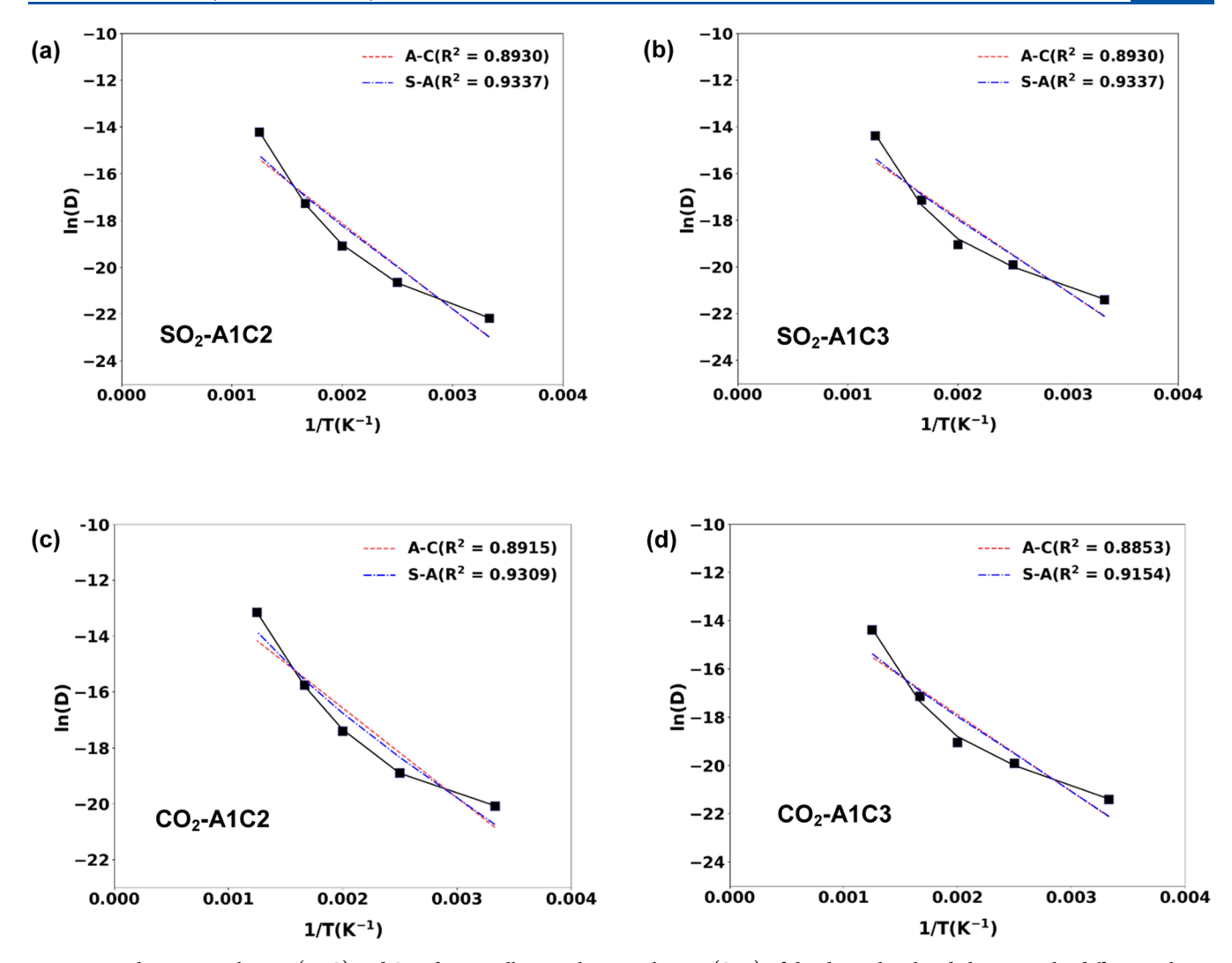


Figure 4. Arrhenius correlations (A, C) and Speedy—Angell power law correlations (S, A) of the thermal scaling behavior in the different solute—solvent systems using a single thermostat for both the solute and solvent. The black squares represent the data points, which are also fitted using a cubic polynomial function (solid black lines).

IL (see Figure S1). These observations suggest that the strong interactions and high solvent viscosities are very difficult to overcome even when the temperature (i.e., kinetic energy) of the solute molecules is significantly elevated. Also, it is clear that the diffusion behavior of the solute molecules in the IL is much more complex than simply traversing a well-defined activation barrier.

3.2. Single Temperature Coupling and the Thermal Scaling Behavior of Diffusivity. A more direct approach is tested next, using a single thermostat to raise the temperature of both the solute and solvent with the intent of developing a predictive scaling relationship. The MSD vs time plots at various temperatures can be found in the Supporting Information (Figures S2–S5). Both an Arrhenius relationship and the Speedy–Angell power law (Figure 4) are used to fit the thermal scaling behavior, which converges more quickly (100–200 ns) at the elevated temperatures explored. The Arrhenius relationship is not able to accurately capture the diffusion behavior, likely because the elevated temperatures distort the diffusion pathways and diffusion mechanisms in the solvent, as these are inherently soft amorphous systems. Likewise, although the power law relationship is moderately

better, the thermal scaling behavior is still not sufficiently captured.

A change in the slope around 1/T = 0.002 can be observed in Figure 4, which also includes a cubic polynomial fit to the data. The self-diffusivities of the ILs (Table S6) help explain the likely cause of this shift. For instance, the diffusivities of the A1 and C2 ions in the CO₂-A1C2 system increase by ~50% from 300 to 500 K, while those of the A1 and C3 ions in the SO_2 -A1C3 system show a ~90% increase from 500 to 600 K. In both systems, the IL diffusivity jumps ~150% from 600 to 800 K, implying a strong temperature influence on the IL diffusion. This underlying shift in IL diffusivity likely influences the CO₂ and SO₂ displacement, e.g., transitioning from localized hopping at lower temperatures to a more classical diffusion at higher temperatures, leading to the observed change in slope. Therefore, using simple Arrhenius-based scaling relationships to predict diffusion across a range of temperatures poses challenges, especially for diverse systems with varying components.

3.3. Thermal Scaling Behavior of the Surface Area and Diffusivity. In an attempt to establish alternative scaling approaches, we evaluated a wide range of other system metrics (e.g., fractional free volume of the solvent, pore size

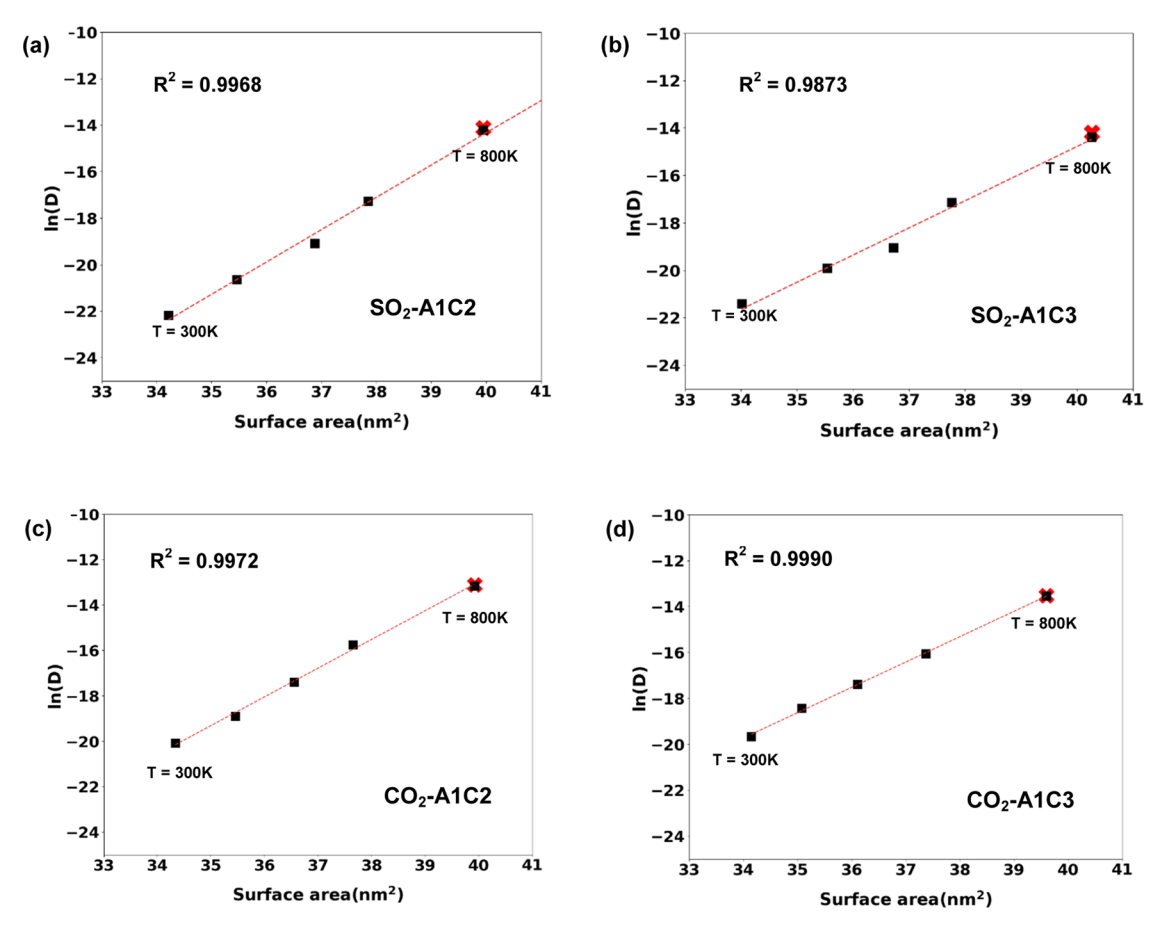


Figure 5. Correlations (dashed lines) of the thermal scaling behavior in the different solute—solvent systems as a function of the solvent surface area, calculated using a probe size of r = 0.075 nm. The points corresponding to the highest and lowest temperatures are indicated. The points marked with red crosses represent the $In(D^{\infty})$ values using the Yeh–Hummer (YH) correction (Figure 7), suggesting minimal influence (<1% difference) of finite size effects on the proposed scaling relationship.

distribution of the solvent, etc.) as a function of temperature. Ultimately, it was found that the accessible surface area of the solvent, calculated over a range of incremental temperatures, is strongly correlated with solute diffusion. The surface area is calculated by tracing the accessible surfaces of the solvent molecules (with diameters defined by the Lennard-Jones parameters of the OPLS force field) using a spherical probe particle. Due to the dynamic nature of the system configurations, 50 different independent snapshots are used to calculate well-converged average solvent surface areas. The results, as shown in Figure 5, indicate a remarkably strong logarithmic correlation between temperature and the solvent surface area, even when different probe sizes are used (Figure 6 shows the optimal probe size as 0.075 nm). This relationship is observed for different solutes (CO₂ and SO₂), as well as different IL solvents (A1C2 and A1C3), implying that the solvent surface area may be a general descriptor for capturing complex diffusion behavior in similar dense, viscous systems.

One possible explanation for this correlation is that the solvent surface area reflects the available space for the solute molecules to move and diffuse. As the temperature increases, the liquid expands, and the surface area increases in a predictable manner, creating more space (or windows between adjacent pockets) for the solute molecules to diffuse. Additionally, the surface area can affect the rate of exchange of solute molecules between the bulk liquid and the surface, which can also influence the diffusion rate. This phenomenon

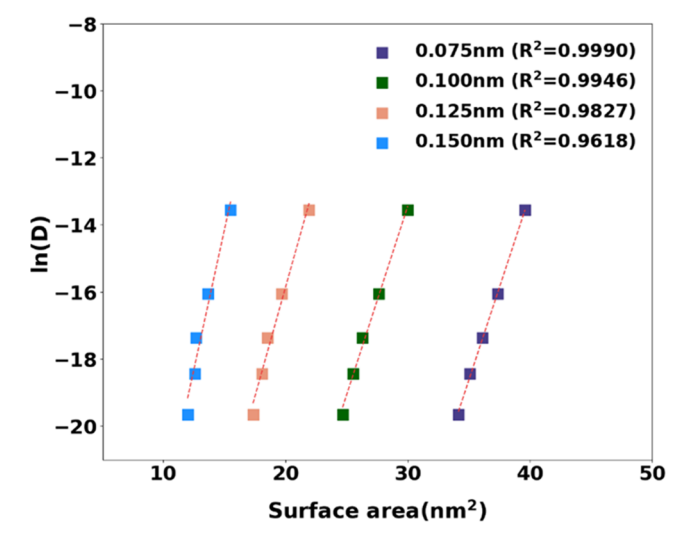


Figure 6. Correlation between solute diffusion and solvent surface area for CO_2 in the A1C3 IL, calculated using different spherical probe radii.

may be related to Danckwerts' surface renewal theory, 76 which expresses the liquid-side mass transfer coefficient ($k_{\rm L}$) in terms of the surface renewal frequency (s) and the molecular diffusivity ($D_{\rm AB}$) of the gas in the liquid:

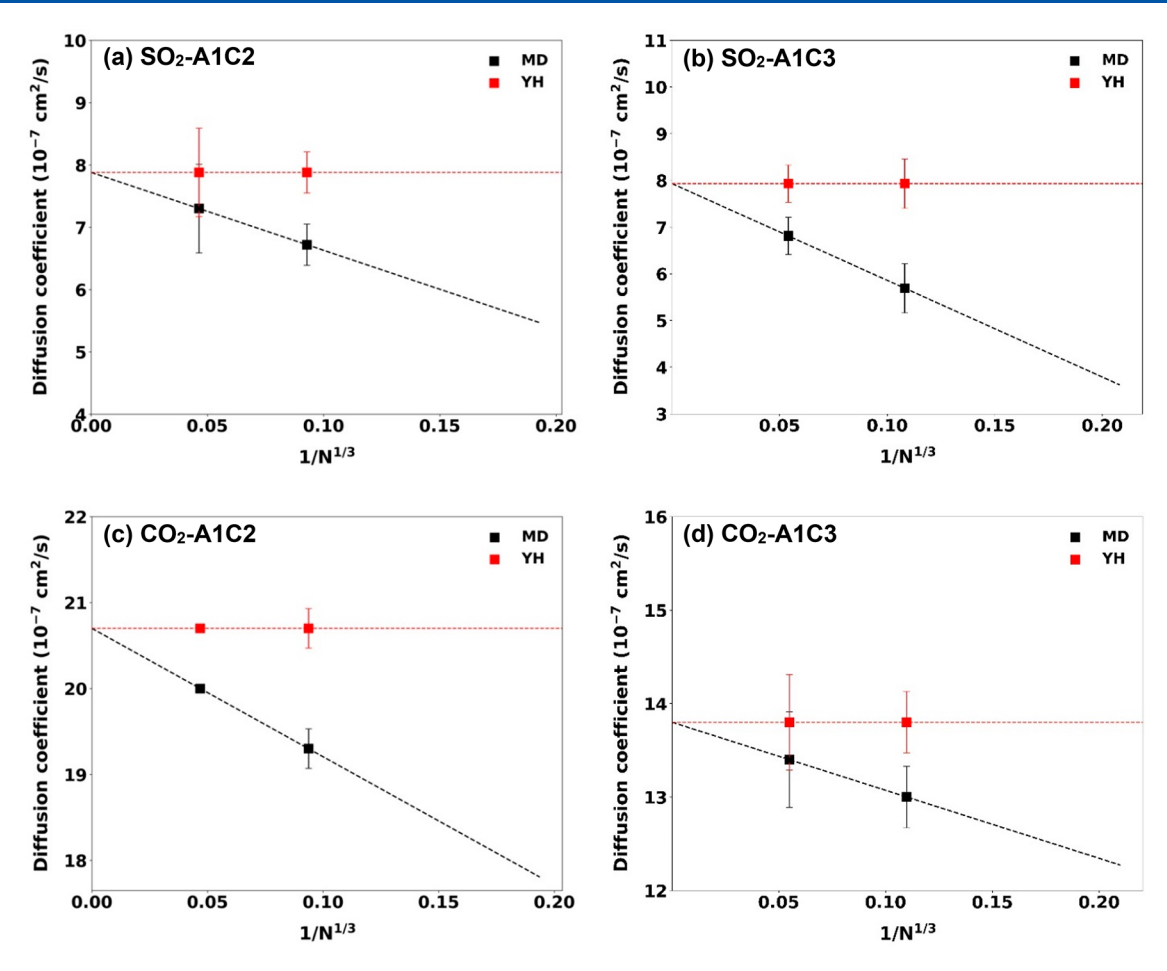


Figure 7. Einstein-derived diffusivity showcases the dependence on the system size. Red squares represent the values of D adjusted by using the Yeh–Hummer (YH) finite size correction, as illustrated in eq 6.

$$k_{\rm L} = (D_{\rm AB}s)^{0.5}$$
 (4)

This theory assumes that the rate of mass transfer between two phases is limited by the rate of surface renewal. In other words, as the surface area of the liquid increases, the rate of surface renewal also increases, which, in turn, can increase the rate of solute diffusion. This concept offers an interesting alternative to the strict Arrhenius hopping, although it does not factor in the expansivity effect.

the expansivity effect.

Other models, ^{77–79} including the free volume theory of solvent diffusivity in polymer solutions, as proposed by Vrentas and Duda, ⁸⁰ do address this expansivity factor. Their model, substantiated by experimental diffusivity data, postulates that the movement of molecules (such as solvents) in a polymer matrix is limited by the availability of free volume. In essence, for a molecule to move, there has to be a sufficient unoccupied volume adjacent to it. The Vrentas—Duda equation is given by eq 5:

$$D = D_0 \exp\left(-\frac{E}{RT}\right) \left(\frac{V_T}{V_1}\right)^{\alpha} \tag{5}$$

where $V_{\rm T}$ and $V_{\rm 1}$ are the free volume fractions of the solvent at the reference and the system temperature, respectively, while α accounts for the concentration-dependent diffusion. The Vrentas–Duda model was primarily designed for polymers; ILs introduce additional complexities due to their ionic nature and specific interactions. However, the fundamental principle

of diffusion being governed by available free spaces (or accessible areas) remains valid. Parameters such as expansivity and solubility that are central to the Vrentas—Duda model could be directly inferred from these simulations. For example, expansivity can be related to how much the accessible surface area expands with temperature, and solubility might dictate how the solute molecules interact with these accessible regions.

Similarly, Paul's free volume theory⁸¹ proposes that, just as with polymers, the accessible surface area in ionic liquids can be seen as a representation of free volume. The solvent-accessible surface area can be interpreted as a metric comparable to free volume (i.e., as the accessible surface area increases, the free volume available for solute molecules should increase as well). Yet, our study indicates that the surface area displays the strongest correlation with diffusion. This could be due to the underlying details of the different systems, especially in ILs with their unique ionic interactions as opposed to conventional synthetic polymers.

To further validate the diffusivity data, it is important to consider finite size effects. This is emphasized by the studies of Celebi et al.⁴⁴ and Jamali et al.,^{43,82} which show the need to correct the diffusivities of both pure components and mixtures for system size effects. For such corrections, the Yeh–Hummer correction⁸³ is commonly used:

$$D^{\infty} = D^{\text{MD}} + \frac{k_{\text{B}} T \varepsilon}{6\pi \eta L} \tag{6}$$

where D^{MD} is the finite self-diffusion coefficient computed in MD simulations, k_{B} is the Boltzmann constant, T is the absolute temperature, η is the shear viscosity computed in MD simulations, and ε is a dimensionless constant equal to 2.837298 for periodic (cubic) lattices. ⁸⁴

Figure 7 plots D^{MD} (obtained from the MSD plots, as shown in Figure S6) against $1/N^{1/3}$, where N denotes the total number of molecules, and the inverse of the simulation box length, L, is directly proportional to $1/N^{1/3}$. The solute diffusion coefficients exhibit a linear relationship with the inverse of the simulation box length; $1/N^{1/3} = 0$ provides the diffusivity value for a system of infinite size (D^{∞}) , which is depicted in the figure as a horizontal line. The corrected diffusivities, taking into account the $\frac{k_{\text{B}}Te}{6\pi\eta L}$ factor from eq 6, are

represented by red squares. As anticipated, these corrected values converge on the horizontal line, reaffirming the accuracy and reliability of the YH correction.

It is also essential to highlight that the finite size effects presented in Figure 7 influence diffusivity results by a maximum of 5–10% at the highest temperature (800 K). The impact would diminish even more at lower temperatures due to the substantial increase in the IL viscosity. Moreover, applying the YH correction to the diffusivity data within the scaling relationship shown in Figure 5 (illustrated by marked cross points at 800 K) on a logarithmic scale reveals a marginal difference (<1%). Thus, in the context of the In *D* vs surface area scaling relationship, the influence of the YH correction is minimal.

Although the mechanistic underpinnings of the diffusive scaling behavior in these ILs are not definitive, the primary advantage of this approach is that the average surface area of the solvent converges very rapidly, even in these dense viscous liquids at room temperature. Therefore, simulations performed at elevated temperatures (requiring relatively short trajectories) can be used to quickly and accurately estimate the solute diffusion at lower temperatures based on a relatively short trajectory at room temperature (needed to estimate the solvent surface area). Although only a few different solvent and solute combinations have been explored in this work, initial results indicate that this method may provide a simple and efficient way for predicting solute diffusion in similar challenging systems.

4. CONCLUSIONS

Here, we studied the diffusion behavior of CO₂ and SO₂ in two multivalent ionic liquids, A1C2 and A1C3, in an attempt to accelerate predictions of solute diffusion in viscous solvents (which otherwise require extremely long MD trajectories). Attempts to improve simulation dynamics via temperature scaling techniques, whether by independently increasing the temperature of the solutes or by raising both solute and solvent temperatures, did not yield satisfactory outcomes. This highlights the complexity of the molecular interactions and solute diffusivity, which does not easily correlate to common scaling relationships. Based on a survey of different physical properties of the solvents, we find a very strong correlation between the solvent-accessible surface area and the diffusion of the solute, as a function of the temperature. This suggests that a solvent's surface area can potentially serve as a key descriptor for predicting complex diffusion behavior in similar dense, viscous systems. This correlation, aligned with Danckwerts' surface renewal theory and the Vrentas-Duda free volume

model, offers an efficient protocol for estimating diffusion behavior using relatively short simulation trajectories performed at elevated temperatures. The precise mechanism underpinning this correlation remains inconclusive and warrants further exploration.

Some of the scaling consistency can be attributed to the fact that CO_2 and SO_2 are both small, rigid solute molecules. However, the outcomes may differ for larger, flexible molecules, potentially presenting weaker correlations or even anomalous behavior, especially with bulkier or more polar solute molecules. Investigating the influence of different solute architectures in future studies will help to clarify the broader applicability of this method. Nonetheless, the approach holds promise for significantly accelerating predictive simulations in challenging comparable systems.

ASSOCIATED CONTENT

5 Supporting Information

The Supporting Information is available free of charge at https://pubs.acs.org/doi/10.1021/acs.jpcb.3c03858.

Gas absorption simulations, surface area, temperature and diffusivity results for the IL systems, Speedy—Angell power law correlations of the thermal scaling behavior in the different solute—solvent systems using a single thermostat for both the solute and solvent, MSDs versus time at various temperatures, and finite size effects (PDF)

Force field parameters for A1; force field parameters for C2; force field parameters for C3; force field parameters for CO₂; force field parameters for SO₂; and the sample input file (PDF)

AUTHOR INFORMATION

Corresponding Author

C. Heath Turner — Department of Chemical and Biological Engineering, The University of Alabama, Tuscaloosa, Alabama 35487-0203, United States; oorcid.org/0000-0002-5707-9480; Phone: 205-348-1733; Email: hturner@eng.ua.edu

Author

Feranmi V. Olowookere — Department of Chemical and Biological Engineering, The University of Alabama, Tuscaloosa, Alabama 35487-0203, United States

Complete contact information is available at: https://pubs.acs.org/10.1021/acs.jpcb.3c03858

Notes

The authors declare no competing financial interest.

ACKNOWLEDGMENTS

We are grateful to the Alabama Supercomputer Authority for computational support. This work is supported by the National Science Foundation EFRI E3P (Award #: 2132133). The authors would like to thank Xiaoyang Liu for providing molecular parameters and initial system configuration files.

REFERENCES

(1) Babu, B.; Shaijumon, M. M. Studies on kinetics and diffusion characteristics of lithium ions in TiNb₂O₇. *Electrochim. Acta* **2020**, 345, No. 136208.

- (2) Zhou, M.; Wang, X.; Zhang, Y.; Qiu, Q.; Liu, M.; Liu, J. Effect of counter diffusion of CO and CO_2 between carbon and anode on the performance of direct carbon solid oxide fuel cells. *Solid State Ionics* **2019**, 343, No. 115127.
- (3) Chen, L.; Liu, D.; Li, Q. CO₂ Diffusivity in H₂O for Supercritical Conditions: A Molecular Dynamics Study. *J. Therm. Sci.* **2022**, *31*, 1407–1415.
- (4) Enyoh, C. E.; Wang, Q.; Wang, W.; Chowdhury, T.; Rabin, M. H.; Islam, R.; Yue, G.; Yichun, L.; Xiao, K. Sorption of Per- and Polyfluoroalkyl Substances (PFAS) using Polyethylene (PE) microplastics as adsorbent: Grand Canonical Monte Carlo and Molecular Dynamics (GCMC-MD) studies. *Int. J. Environ. Anal. Chem.* 2022, 1–17, DOI: 10.1080/03067319.2022.2070016.
- (5) Islam, M. Z.; Hossain, S. I.; Deplazes, E.; Bhowmick, S.; Saha, S. C. Molecular dynamics study of prednisolone concentration on cholesterol based lung surfactant monolayer. *AIP Conf. Proc.* **2021**, 2324, No. 060008, DOI: 10.1063/5.0037471.
- (6) Salo-Ahen, O. M. H.; Alanko, I.; Bhadane, R.; Bonvin, A. M. J. J.; Honorato, R. V.; Hossain, S.; Juffer, A. H.; Kabedev, A.; Lahtela-Kakkonen, M.; Larsen, A. S.; et al. Molecular Dynamics Simulations in Drug Discovery and Pharmaceutical Development. *Processes* **2021**, *9*, 71.
- (7) Maleki, R.; Shams, S. M.; Chellehbari, Y. M.; Rezvantalab, S.; Jahromi, A. M.; Asadnia, M.; Abbassi, R.; Aminabhavi, T.; Razmjou, A. Materials discovery of ion-selective membranes using artificial intelligence. *Commun. Chem.* **2022**, *5*, 132.
- (8) Bukowski, B. C.; Keil, F. J.; Ravikovitch, P. I.; Sastre, G.; Snurr, R. Q.; Coppens, M.-O. Connecting theory and simulation with experiment for the study of diffusion in nanoporous solids. *Adsor* **2021**, *27*, 683–760.
- (9) Shang, Y.; Kundu, D. Understanding and Performance of the Zinc Anode Cycling in Aqueous Zinc-Ion Batteries and a Roadmap for the Future. *Batteries Supercaps* **2022**, *5*, No. e202100394, DOI: 10.1002/batt.202100394.
- (10) Asensio-Delgado, S.; Pardo, F.; Zarca, G.; Urtiaga, A. Vapor–Liquid Equilibria and Diffusion Coefficients of Difluoromethane, 1,1,1,2-Tetrafluoroethane, and 2,3,3,3-Tetrafluoropropene in Low-Viscosity Ionic Liquids. *J. Chem. Eng. Data* **2020**, *65*, 4242–4251.
- (11) Shokouhi, M.; Sakhaeinia, H.; Jalili, A. H.; Zoghi, A. T.; Mehdizadeh, A. Experimental diffusion coefficients of CO_2 and H_2S in some ionic liquids using semi-infinite volume method. *J. Chem. Thermodyn.* **2019**, *133*, 300–311.
- (12) Delgado-Mellado, N.; Ayuso, M.; García, J.; Rodríguez, F. Aliphatic and aromatic hydrocarbon diffusion coefficients at infinite dilution in [emim][DCA] and [4empy][Tf₂N] ionic liquids. *J. Mol. Liq.* 2019, 288, No. 111082.
- (13) Friedrich, M. F.; Kokolakis, S.; Lucas, M.; Claus, P. Measuring Diffusion and Solubility of Slightly Soluble Gases in [CnMIM][NTf₂] Ionic Liquids. *J. Chem. Eng. Data* **2016**, *61*, 1616–1624.
- (14) Camper, D.; Becker, C.; Koval, C.; Noble, R. Diffusion and Solubility Measurements in Room Temperature Ionic Liquids. *Ind. Eng. Chem. Res.* **2006**, *45*, 445–450.
- (15) Lei, Z.; Dai, C.; Chen, B. Gas Solubility in Ionic Liquids. *Chem. Rev.* **2014**, *114*, 1289–1326.
- (16) Haider, J.; Saeed, S.; Qyyum, M. A.; Kazmi, B.; Ahmad, R.; Muhammad, A.; Lee, M. Simultaneous capture of acid gases from natural gas adopting ionic liquids: Challenges, recent developments, and prospects. *Renewable Sustainable Energy Rev.* **2020**, *123*, No. 109771.
- (17) Zhang, W.; Liu, X.; Zhang, H.; Li, S.; Yang, J.; Cui, P.; Zhu, Z.; Ma, Y.; Wang, Y. Molecular Dynamics Evaluation of Removal of Acid Gases from SNG by Ionic Liquid. ACS Sustainable Chem. Eng. 2019, 7, 18093–18104.
- (18) Reddy, T. D. N.; Mallik, B. S. Ionic Dynamics of Hydroxylammonium Ionic Liquids: A Classical Molecular Dynamics Simulation Study. *J. Phys. Chem. B* **2020**, *124*, 4960–4974.
- (19) Figueiredo, N. M.; Voroshylova, I. V.; Koverga, V. A.; Ferreira, E. S. C.; Cordeiro, M. N. D. S. Influence of alcohols on the inter-ion

- interactions in ionic liquids: A molecular dynamics study. *J. Mol. Liq.* **2019**, 294, No. 111538.
- (20) Jahanbakhsh-Bonab, P.; Sardroodi, J. J.; Avestan, M. S. Electric Field Effects on the Structural and Dynamical Properties of a Glyceline Deep Eutectic Solvent. *J. Chem. Eng. Data* **2022**, *67*, 2077—2087.
- (21) Tsuzuki, S.; Shinoda, W.; Saito, H.; Mikami, M.; Tokuda, H.; Watanabe, M. Molecular Dynamics Simulations of Ionic Liquids: Cation and Anion Dependence of Self-Diffusion Coefficients of Ions. *J. Phys. Chem. B* **2009**, *113*, 10641–10649.
- (22) Graham, T. I. The Bakerian Lecture.—On the diffusion of liquids. *Philos. Trans. R. Soc. London* **1850**, 140, 1–46, DOI: 10.1098/rstl.1850.0001.
- (23) Fick, A. V. On liquid diffusion. London, Edinburgh Dublin Philos. Mag. J. Sci. 1855, 10, 30–39, DOI: 10.1080/14786445508641925.
- (24) Evans, R. The interpretation of small molecule diffusion coefficients: Quantitative use of diffusion-ordered NMR spectroscopy. *Prog. Nucl. Magn. Reson. Spectrosc.* **2020**, *117*, 33–69.
- (25) Peters, C.; Wolff, L.; Haase, S.; Thien, J.; Brands, T.; Koß, H.-J.; Bardow, A. Multicomponent diffusion coefficients from microfluidics using Raman microspectroscopy. *Lab Chip* **2017**, *17*, 2768–2776.
- (26) Zhang, C.; Jin, Z.; Zeng, B.; Wang, W.; Palui, G.; Mattoussi, H. Characterizing the Brownian Diffusion of Nanocolloids and Molecular Solutions: Diffusion-Ordered NMR Spectroscopy vs Dynamic Light Scattering. *J. Phys. Chem. B* **2020**, *124*, 4631–4650.
- (27) Hopp, M.; Mele, J.; Gross, J. Self-Diffusion Coefficients from Entropy Scaling Using the PCP-SAFT Equation of State. *Ind. Eng. Chem. Res.* **2018**, *57*, 12942–12950.
- (28) Wilke, C. R.; Chang, P. Correlation of diffusion coefficients in dilute solutions. *AIChE J.* **1955**, *1*, 264–270.
- (29) Edward, J. T. Molecular volumes and the Stokes-Einstein equation. J. Chem. Educ. 1970, 47, 261.
- (30) Keaveney, S. T.; Schaffarczyk McHale, K. S.; Stranger, J. W.; Ganbold, B.; Price, W. S.; Harper, J. B. NMR Diffusion Measurements as a Simple Method to Examine Solvent—Solvent and Solvent—Solute Interactions in Mixtures of the Ionic Liquid [Bmim][N(SO₂CF₃)₂] and Acetonitrile. *ChemPhysChem* **2016**, *17*, 3853—3862.
- (31) Tsimpanogiannis, I. N.; Moultos, O. A. Is Stokes-Einstein relation valid for the description of intra-diffusivity of hydrogen and oxygen in liquid water? *Fluid Phase Equilib.* **2023**, 563, No. 113568.
- (32) Tsimpanogiannis, I. N.; Jamali, S. H.; Economou, I. G.; Vlugt, T. J. H.; Moultos, O. A. On the validity of the Stokes–Einstein relation for various water force fields. *Mol. Phys.* **2020**, *118*, No. e1702729.
- (33) Moultos, O. A.; Tsimpanogiannis, I. N. Predictive model for the intra-diffusion coefficients of H_2 and O_2 in vapour H_2O based on data from molecular dynamics simulations. *Mol. Phys.* **2023**, No. e2211889, DOI: 10.1080/00268976.2023.2211889.
- (34) Tsimpanogiannis, I. N.; Maity, S.; Celebi, A. T.; Moultos, O. A. Engineering Model for Predicting the Intradiffusion Coefficients of Hydrogen and Oxygen in Vapor, Liquid, and Supercritical Water based on Molecular Dynamics Simulations. *J. Chem. Eng. Data* **2021**, *66*, 3226–3244.
- (35) Wolff, L.; Jamali, S. H.; Becker, T. M.; Moultos, O. A.; Vlugt, T. J. H.; Bardow, A. Prediction of Composition-Dependent Self-Diffusion Coefficients in Binary Liquid Mixtures: The Missing Link for Darken-Based Models. *Ind. Eng. Chem. Res.* **2018**, *57*, 14784–14794.
- (36) McCarty, K. P.; Mason, E. A. Kirkendall effect in gaseous diffusion. *Phys. Fluids* **1960**, *3*, 908–922.
- (37) Aghaie, M.; Rezaei, N.; Zendehboudi, S. New insights into bulk and interface properties of [Bmim][Ac]/[Bmim][BF4] ionic liquid/ CO₂ systems Molecular dynamics simulation approach. *J. Mol. Liq.* **2020**, 317, No. 113497.
- (38) Guo, Q.; Liu, Q.; Zhao, Y. Insights into the Structure and Dynamics of Imidazolium Ionic Liquid and Tetraethylene Glycol Dimethyl Ether Cosolvent Mixtures: A Molecular Dynamics Approach. *Nanomaterials* **2021**, *11*, 2512.

- (39) Allen, M. P.; Tildesley, D. J. Computer Simulation of Liquids; Oxford university press, 2017; pp 73–79.
- (40) Cappelezzo, M.; Capellari, C. A.; Pezzin, S. H.; Coelho, L. A. F. Stokes-Einstein relation for pure simple fluids. *J. Chem. Phys.* **2007**, 126, No. 224516, DOI: 10.1063/1.2738063.
- (41) Moradi, M.; Azizpour, H.; Mohammarehnezhad-Rabieh, M. Determination of diffusion coefficient of C₂H₆ and CO₂ in hydrocarbon solvents by molecular dynamics simulation. *J. Mol. Liq.* **2023**, *370*, No. 121015.
- (42) Santos, J. R. C.; Abreu, P. E.; Marques, J. M. C. Calculation of diffusion coefficients of pesticides by employing molecular dynamics simulations. *J. Mol. Liq.* **2021**, 340, No. 117106.
- (43) Jamali, S. H.; Wolff, L.; Becker, T. M.; Bardow, A.; Vlugt, T. J. H.; Moultos, O. A. Finite-Size Effects of Binary Mutual Diffusion Coefficients from Molecular Dynamics. *J. Chem. Theory and Comp.* **2018**, *14*, 2667–2677.
- (44) Celebi, A. T.; Jamali, S. H.; Bardow, A.; Vlugt, T. J. H.; Moultos, O. A. Finite-size effects of diffusion coefficients computed from molecular dynamics: a review of what we have learned so far. *Mol. Simul.* **2021**, *47*, 831–845.
- (45) Figueiredo, N. M.; Voroshylova, I. V.; Koverga, V. A.; Ferreira, E. S.; Cordeiro, M. N. D. Influence of alcohols on the inter-ion interactions in ionic liquids: A molecular dynamics study. *J. Mol. Liq.* **2019**, 294, No. 111538.
- (46) Woo, Y.; Pérez-Rodríguez, M.; Jeong, J. H.; Piñeiro, M. M.; Lee, J.-W.; Lee, Y.; Jung, S.-H.; Kim, H.; Takeya, S.; Yamamoto, Y.; et al. Extremely Slow Diffusion of Argon Atoms in Clathrate Cages: Implications for Gas Storage in Solid Materials. *ACS Sustainable Chem. Eng.* **2021**, *9*, 7479–7488.
- (47) Rodríguez-García, B.; Piñeiro, M. M.; Pérez-Rodríguez, M. Diffusion and dynamics of noble gases in hydroquinone clathrate channels. *J. Chem. Phys.* **2023**, *158*, No. 044503, DOI: 10.1063/5.0137734.
- (48) Pramanik, K.; Borah, S.; Kumar, P. P. Accessing slow diffusion in solids by employing metadynamics simulation. *Phys. Chem. Chem. Phys.* **2020**, 22, 22796–22804.
- (49) Heelweg, H. J.; De Souza, R. A. Metadynamics simulations of strontium-vacancy diffusion in SrTiO₃. *Phys. Rev. Mater.* **2021**, *5*, No. 013804
- (50) Camp, J. S.; Sholl, D. S. Transition State Theory Methods To Measure Diffusion in Flexible Nanoporous Materials: Application to a Porous Organic Cage Crystal. *J. Phys. Chem. C* **2016**, *120*, 1110–1120.
- (51) de Oliveira, C. A. F.; Hamelberg, D.; McCammon, J. A. On the Application of Accelerated Molecular Dynamics to Liquid Water Simulations. *J. Phys. Chem. B* **2006**, *110*, 22695–22701.
- (52) Ebina, H.; Fukuhara, S.; Shibuta, Y. Accelerated molecular dynamics simulation of vacancy diffusion in substitutional alloy with collective variable-driven hyperdynamics. *Comput. Mater. Sci.* **2021**, 196, No. 110577.
- (53) Abe, Y. Application of hyper-molecular dynamics to self-interstitial diffusion in α -iron. *Comput. Mater. Sci.* **2013**, 74, 23–26.
- (54) Li, H.; Min, D.; Liu, Y.; Yang, W. Essential energy space random walk via energy space metadynamics method to accelerate molecular dynamics simulations. *J. Chem. Phys.* **2007**, 127, No. 094101, DOI: 10.1063/1.2769356.
- (55) Hussain, S.; Haji-Akbari, A. Studying rare events using forward-flux sampling: Recent breakthroughs and future outlook. *J. Chem. Phys.* **2020**, *152*, No. 060901.
- (56) Kundu, N.; Roy, A.; Dutta, R.; Sarkar, N. Translational and Rotational Diffusion of Two Differently Charged Solutes in Ethylammonium Nitrate—Methanol Mixture: Does the Nanostructure of the Amphiphiles Influence the Motion of the Solute? *J. Phys. Chem. A* **2016**, *120*, 5481–5490.
- (57) Araque, J. C.; Yadav, S. K.; Shadeck, M.; Maroncelli, M.; Margulis, C. J. How Is Diffusion of Neutral and Charged Tracers Related to the Structure and Dynamics of a Room-Temperature Ionic Liquid? Large Deviations from Stokes—Einstein Behavior Explained. *J. Phys. Chem. B* **2015**, *119*, 7015—7029.

- (58) Moya, C.; Palomar, J.; Gonzalez-Miquel, M.; Bedia, J.; Rodriguez, F. Diffusion Coefficients of CO₂ in Ionic Liquids Estimated by Gravimetry. *Ind. Eng. Chem. Res.* **2014**, *53*, 13782–13789.
- (59) Stephens, N. M.; Masching, H. P.; Walid, M. K. I.; Petrich, J. W.; Anderson, J. L.; Smith, E. A. Temperature-Dependent Constrained Diffusion of Micro-Confined Alkylimidazolium Chloride Ionic Liquids. *J. Phys. Chem. B* **2022**, *126*, 4324–4333.
- (60) Ahosseini, A.; Ren, W.; Weatherley, L. R.; Scurto, A. M. Viscosity and self-diffusivity of ionic liquids with compressed hydrofluorocarbons: 1-Hexyl-3-methyl-imidazolium bis-(trifluoromethylsulfonyl)amide and 1,1,1,2-tetrafluoroethane. *Fluid Phase Equilib.* **2017**, 437, 34–42, DOI: 10.1016/j.fluid.2016.11.022.
- (61) Speedy, R. J.; Angell, C. A. Isothermal compressibility of supercooled water and evidence for a thermodynamic singularity at 45°C. J. Chem. Phys. 1976, 65, 851–858.
- (62) Dahl, S.; Fredenslund, A.; Rasmussen, P. The MHV2 model: a UNIFAC-based equation of state model for prediction of gas solubility and vapor-liquid equilibria at low and high pressures. *Ind. Eng. Chem. Res.* **1991**, *30*, 1936–1945.
- (63) Pablo, G. D. Supercooled and glassy water. *J. Phys.: Condens. Matter* **2003**, *15*, R1669 DOI: 10.1088/0953-8984/15/45/R01.
- (64) Liu, X.; O'Harra, K. E.; Bara, J. E.; Turner, C. H. Molecular insight into the anion effect and free volume effect of CO₂ solubility in multivalent ionic liquids. *Phys. Chem. Chem. Phys.* **2020**, 22, 20618–20633.
- (65) Liu, X.; Turner, C. H. Quantifying the anion effect of gas solubility within ionic liquids using the solvation affinity index. *Chem. Eng. Sci.* **2022**, *260*, No. 117851.
- (66) Martínez, L.; Andrade, R.; Birgin, E. G.; Martínez, J. M. PACKMOL: A package for building initial configurations for molecular dynamics simulations. *J. Comput. Chem.* **2009**, *30*, 2157–2164.
- (67) Abraham, M. J.; Murtola, T.; Schulz, R.; Páll, S.; Smith, J. C.; Hess, B.; Lindahl, E. GROMACS: High performance molecular simulations through multi-level parallelism from laptops to supercomputers. *SoftwareX* **2015**, *1*, 19–25, DOI: 10.1016/j.softx.2015.06.001.
- (68) Robertson, M. J.; Tirado-Rives, J.; Jorgensen, W. L. Improved peptide and protein torsional energetics with the OPLS-AA force field. *J. Chem. Theory Comput.* **2015**, *11*, 3499–3509.
- (69) Dodda, L. S.; Cabeza de Vaca, I.; Tirado-Rives, J.; Jorgensen, W. L. LigParGen web server: an automatic OPLS-AA parameter generator for organic ligands. *Nucleic Acids Res.* **2017**, *45*, W331–W336
- (70) Potoff, J. J.; Siepmann, J. I. Vapor—liquid equilibria of mixtures containing alkanes, carbon dioxide, and nitrogen. *AIChE J.* **2001**, *47*, 1676—1682.
- (71) Ketko, M. H.; Kamath, G.; Potoff, J. J. Development of an optimized intermolecular potential for sulfur dioxide. *J. Phys. Chem. B* **2011**, *115*, 4949–4954.
- (72) Hoover, W. G. Canonical dynamics: Equilibrium phase-space distributions. *Phys. Rev. A* 1985, 31, 1695.
- (73) Parrinello, M.; Rahman, A. Crystal structure and pair potentials: A molecular-dynamics study. *Phys. Rev. Lett.* **1980**, *45*, 1196.
- (74) Darden, T.; York, D.; Pedersen, L. Particle mesh Ewald: An Nlog (N) method for Ewald sums in large systems. *J. Chem. Phys.* **1993**, 98, 10089–10092.
- (75) Hess, B.; Bekker, H.; Berendsen, H. J.; Fraaije, J. G. LINCS: A linear constraint solver for molecular simulations. *J. Comput. Chem.* **1997**, *18*, 1463–1472.
- (76) Danckwerts, P. V. Significance of Liquid-Film Coefficients in Gas Absorption. *Ind. Eng. Chem.* **1951**, 43, 1460–1467.
- (77) Yasuda, H.; Lamaze, C. E.; Ikenberry, L. D. Permeability of solutes through hydrated polymer membranes. Part I. Diffusion of sodium chloride. *Makromol. Chem.* **1968**, *118*, 19–35.
- (78) Kumins, C.; Kwei, T. Diffusion in Polymers; Academic Press: New York, NY, 1968; pp 135–137.

- (79) Zielinski, J. M.; Duda, J. L. Predicting polymer/solvent diffusion coefficients using free-volume theory. *AIChE J.* **1992**, 38, 405–415
- (80) Vrentas, J.; Duda, J.; Ling, H. C.; Hou, A. C. Free-volume theories for self-diffusion in polymer—solvent systems. II. Predictive capabilities. *J. Polym. Sci., Part B: Polym. Phys.* **1985**, 23, 289–304.
- (81) Paul, D. Gas transport in homogeneous multicomponent polymers. J. Membr. Sci. 1984, 18, 75–86.
- (82) Jamali, S. H.; Bardow, A.; Vlugt, T. J.; Moultos, O. A. Generalized form for finite-size corrections in mutual diffusion coefficients of multicomponent mixtures obtained from equilibrium molecular dynamics simulation. *J. Chem. Theory Comput.* **2020**, *16*, 3799–3806.
- (83) Yeh, I.-C.; Hummer, G. System-size dependence of diffusion coefficients and viscosities from molecular dynamics simulations with periodic boundary conditions. *J. Phys. Chem. B* **2004**, *108*, 15873–15879.
- (84) Kikugawa, G.; Ando, S.; Suzuki, J.; Naruke, Y.; Nakano, T.; Ohara, T. Effect of the computational domain size and shape on the self-diffusion coefficient in a Lennard-Jones liquid. *J. Chem. Phys.* **2015**, *142*, No. 024503, DOI: 10.1063/1.4905545.